Pemetrexed increases BRCA1 protein stability and sensitizes TNBC cells to radiotherapy

HEE JIN[1*], KYUNG-HWA JEON[1*], CHAERIN KANG[1], JOOHYUN LEE[1], YEONJIN LEE[2], YOUNGJOO KWON[1,2] and YUN-SIL LEE[1,2]

[1]Graduate School of Pharmaceutical Sciences and College of Pharmacy, Ewha Womans University, Seoul 03760, Republic of Korea; [2]Innovative BioPharmChem Convergence Education and Research Program, Ewha Womans University, Seoul 03760, Republic of Korea

Received February 10, 2026; Accepted August 19, 2026

DOI: 10.3892/or.2026.9194

Abstract. BRCA1 is a multifunctional tumor suppressor that orchestrates homologous recombination repair, chromatin remodeling, cell cycle control and apoptosis. Although pathogenic BRCA1 mutations are relatively uncommon, decreased BRCA1 protein expression, which is typically driven by accelerated proteasomal degradation, is implicated in aggressive breast cancer (BC), particularly triple-negative (TN)BC. These mutations may modulate therapeutic response to DNA-damaging agents. Given the absence of clinically available strategies to restore BRCA1 stability, the present study evaluated whether pemetrexed (Peme), a multitargeted antifolate identified through an *in silico* US Food and Drug Administration-approved drug screen, modulates BRCA1 protein homeostasis in TNBC models. BRCA1 protein abundance, ubiquitination and turnover were assessed using immunoblotting, ubiquitin pull-down and cycloheximide chase analyses and BRCA1 domain mutants. Functional consequences of Peme treatment were measured by apoptosis assay and BRCA1-dependent signaling readouts. The radiosensitizing effect of Peme was evaluated *in vitro* and validated in TNBC xenografts. Peme increased BRCA1 protein levels without altering BRCA1 mRNA, indicating post-translational regulation. Mechanistically, *in silico* docking and BRCA1 deletion mutant analyses suggested that the BRCA1 C-terminal domain may contribute to the effect of Peme on BRCA1 stability, suppressing ubiquitin-mediated proteasomal degradation and resulting in protein stabilization. Stabilized BRCA1 enhanced apoptotic responses, whereas BRCA1 knockdown attenuated these effects. Combined Peme-radiation treatment significantly potentiated cytotoxicity *in vitro* and inhibited tumor growth *in vivo*, demonstrating a radiosensitizing effect linked to BRCA1 stabilization. Collectively, these findings identified Peme as a BRCA1-stabilizing agent that enhances therapeutic response to radiation in TNBC. Pharmacological restoration of BRCA1 stability represents a promising strategy to overcome therapeutic resistance in BRCA1-deficient or functionally compromised BC.

Introduction

BRCA1 serves multifaceted roles in maintaining genomic stability, including homologous recombination (HR)-mediated DNA repair, cell cycle regulation, ubiquitin ligase activity, chromatin remodeling and apoptosis induction (1,2). Germline pathogenic variants in BRCA1 predispose individuals to hereditary ovarian and breast cancer (BC) by compromising its tumor suppressor function (3,4). While germline BRCA1 mutations are recognized in familial cancer syndromes, loss or downregulation of wild-type BRCA1 protein is also evident in sporadic BC (1).

In triple-negative (TN)BC, BRCA1 downregulation is particularly relevant. Some studies report that up to ~30% of patients with TNBC exhibit reduced BRCA1 expression, which is associated with more aggressive disease behavior and poorer prognosis (1,5,6). For example, Irianiwati *et al* (7) showed that negative BRCA1 immunostaining is associated with more advanced TNBC tumor stage, although it did not independently predict survival outcomes.

Functionally, increased BRCA1 levels are linked to augmented apoptosis in BC models exposed to stressors, including DNA damage, ionizing radiation (IR) and chemotherapeutic agents (8,9). BRCA1 activates apoptosis-promoting pathways, for example, through p53-dependent transcriptional programs, activation of the MEKK4/JNK signaling cascades, interaction with the Fas receptor pathway, growth arrest and DNA damage-inducible 45 (GADD45)-mediated nuclear export leading to JNK activation, inositol 1,4,5-trisphosphate receptor-mediated calcium flux, modulation of estrogen

Correspondence to: Professor Youngjoo Kwon or Professor Yun-Sil Lee, Graduate School of Pharmaceutical Sciences and College of Pharmacy, Ewha Womans University, Pharmacy Building B, Room 214, 52 Ewhayeodae, Seodaemun, Seoul 03760, Republic of Korea
E-mail: ykwon@ewha.ac.kr
E-mail: yslee0425@ewha.ac.kr

*Contributed equally

Key words: BRCA1, triple-negative breast cancer, pemetrexed, protein stability, radiosensitization

receptor α and proteasomal degradation of the anti-apoptotic BCL2 in the cytoplasm (9-12). Therefore, restoring proper BRCA1 localization and function, particularly within the cytoplasmic compartment, represents a potential strategy to sensitize tumor cells to radiation and to promote apoptosis.

At the posttranslational level, BRCA1 expression is regulated by the ubiquitin-proteasome degradation pathway (13,14). Ubiquitin conjugates that target BRCA1 for proteasomal targeting are distinct from its auto-ubiquitination products, suggesting that other E3 ligases may be involved (15-17). BRCA1-associated RING domain protein 1 (BARD1), a well-characterized BRCA1 binding partner, stabilizes BRCA1 by suppressing its proteasome-sensitive ubiquitination; reciprocally, elevated BRCA1 upregulates BARD1 expression, forming a positive feedback loop (18-20). Several E3 ligases, including HECT and RLD domain containing E3 ubiquitin protein ligase 2 (HERC2), HECT, UBA and WWE domain containing E3 ubiquitin protein ligase 1 (HUWE1), F-box protein 44 (FBXO44) and Parkin, have been implicated in BRCA1 turnover (16,17,21,22). Cathepsin S (CTSS), a lysosomal cysteine protease, is an enzyme that cleaves the BRCA1 C-terminal (BRCT) domain of BRCA1, triggering ubiquitination and proteasomal degradation. Inhibiting CTSS rescues BRCA1 levels and suppresses tumor growth (12,14,23).

Furthermore, the integrity of the BRCA1-BARD1 heterodimer is key for BRCA1 stabilization. Factors such as SIRT2, p53-responsive long non-coding RNA GUARDIN and tumor suppressor candidate 4 stabilize the BRCA1-BARD1 complex, whereas ubiquitin-conjugating enzyme E2 T and transforming acidic coiled-coil containing protein 3 (TACC3) destabilize it, thereby promoting BRCA1 degradation (10,24). Nevertheless, because BRCA1 can undergo proteasomal degradation independently of BARD1 interaction, the process may be regulated by multiple pathways (15,25).

Therapeutically, poly-ADP-ribose polymerase (PARP) inhibitors such as olaparib exploit HR deficiency, particularly in tumors harboring mutated or nonfunctional BRCA1. Olaparib traps PARP1 on DNA, thereby exacerbating double-strand break burden that HR-deficient cells cannot properly repair (26,27). However, in BC that retains wild-type BRCA1 but exhibits low expression or stability, there are currently no approved targeted therapies specifically designed to restore BRCA1 function or stability.

Pemetrexed (Peme) is a multitargeted antifolate agent approved for non-squamous non-small cell lung cancer (NSCLC) and malignant pleural mesothelioma. It inhibits key enzymes involved in nucleotide biosynthesis, such as thymidylate synthase, dihydrofolate reductase and glycinamide ribonucleotide formyl transferase (28,29). Although primarily used for lung cancer, a randomized phase II clinical trial demonstrated that a Peme-containing neoadjuvant regimen is active and generally well tolerated in patients with early BC (30). Moreover, liposomal formulations of Peme have demonstrated favorable tolerability and activity in metastatic BC (31-33).

The present study aimed to investigate the effects of Peme on BRCA1 protein stability and its underlying regulatory mechanism, as well as to evaluate its potential to enhance radiosensitivity in TNBC.

Materials and methods

Cell culture. Human TNBC cell lines MDA-MB-231 (American Type Culture Collection) and HCC70 (Korean Cell Line Bank), both harboring wild-type BRCA1, were cultured in RPMI-1640 medium (cat. no. LM011-01; Welgene, Inc.) and DMEM (cat no. LM001-05; Welgene, Inc.), respectively. The media were supplemented with 10% fetal bovine serum (FBS; cat. no. 35-015-CV; Gibco; Thermo Fisher Scientific, Inc.), 0.1 mM non-essential amino acids (cat. no. LS005-01; Welgene, Inc.), glutamine (cat. no. 25030081), HEPES (cat. no. 15630080; both Gibco; Thermo Fisher Scientific, Inc.) and antibiotics (cat. no. CA005-010; GenDEPOT) at 37˚C in a 5% CO_2 humidified incubator.

Compounds and chemicals. E-64 (cat. no. E3132) and MG132 (cat. no. M7449) were purchased from Sigma-Aldrich (Merck KGaA) and ZFL-COCHO (ZFL; cat. no. A13502) was purchased from AdooQ Bioscience LLC. Venetoclax (cat. no. S8048), sofosbuvir (cat. no. S2794), silodosin (cat. no. S1613), candesartan cilexetil (cat. no. S2037), sodium phenylbutyrate (cat. no. S4125), tirofiban (cat. no. S3085) and bimatoprost (cat. no. S1407) were purchased from Selleck Chemicals. Olodaterol (cat. no. CS-6275) and Peme (cat. no. CS-1297) were obtained from ChemScene LLC. RO5461111 (RO; cat. no. HY-114374) was purchased from MedChemExpress. MDA-MB-231 cells were treated with venetoclax, sofosbuvir, olodaterol, silodosin, candesartan, Peme, sodium phenylbutyrate, tirofiban or bimatoprost at 5 μM for 24 h at 37˚C, with E-64 (5 μM) included as a positive control. BRCA1 and CTSS protein expression was subsequently analyzed by western blotting.

Antibodies. BRCA1 (C-20; C-terminal epitope; cat. no. SC-642), BRCA1 (cat. no. SC-6954), PARP (cat. no. SC-8007) and β-actin (all 1:1,000; cat. no. SC-47778) antibodies were purchased from Santa Cruz Biotechnology, Inc. Cleaved PARP (1:1,000; cat. no. 9541), anti-cleaved caspase-3 (cat. no. 9661), anti-caspase-3 (cat. no. 9662), anti-Histidine tag (His-tag; cat. no. 2365), anti-Lamin A/C (cat. no. 2032), anti-CTSS (all 1:1,000; cat. no. 25084) antibodies were purchased from Cell signaling Technology, Inc. Monoclonal FLAG M2 (1:1,000; cat. no. F3165) was purchased from Sigma-Aldrich (Merck KGaA). Anti-Ki-67 (1:200; cat. no. M7240) was obtained from Dako (Agilent Technologies, Inc.).

BRCA1 plasmid constructs. Wild-type BRCA1 (WT-BRCA1) and BRCA1 deletion constructs lacking the RING (ΔRING) or BRCT (ΔBRCT) domain were generated as described previously (14) using human breast cDNA as a template and cloned into mammalian expression vectors pcDNA3.1 (Invitrogen; Thermo Fisher Scientific, Inc.) and p3xFLAG-myc-CMV-23 (cat. no. E9158; Sigma-Aldrich; Merck KGaA). The WT-BRCA1, ΔRING and ΔBRCT constructs were transfected into 293T cells for immunoblotting and GADD45 promoter assays.

Cell transfection. Cells were seeded at a density $3x10^5$ cells/dish in 60 mm culture dishes, and transfection was performed after 24 h using Opti-MEM (cat. no. 31985070; Gibco; Thermo Fisher Scientific, Inc.) containing Transfex transfection reagent

(cat. no. ACS-4005; American Type Culture Collection). For small interfering (si)RNA-mediated BRCA1 knockdown, SignalSilence® BRCA1 siRNA I (cat. no. 12519) and SignalSilence® Control siRNA (Unconjugated; cat. no. 6568; both Cell Signaling Technology, Inc.) were transfected at a final concentration of 100 nM for 24 h at 37˚C, according to the manufacturer's instructions. The siRNA sequences were not provided by the supplier. Cells were collected for subsequent analysis 48 h after transfection.

MTT assay. Cell viability following treatment with RO, ZFL, candesartan or Peme was evaluated using an MTT (cat. no. 475989; Sigma-Aldrich; Merck KGaA) assay. MDA-MB-231 cells were seeded into 96-well plates at a density of $1x10^4$ cells/well and allowed to attach overnight. Cells were treated with RO, Z-FL-COCHO, candesartan or Peme at concentrations of 10, 25, 50 and 100 μM for 24 h at 37˚C. Subsequently, cells were incubated with 100 μl MTT solution (5 mg/ml) for 4 h at 37˚C. The MTT solution was removed and 100 μl DMSO was added to each well to dissolve the formazan crystals. Absorbance was measured at 540 nm using a microplate reader (Tecan Group Limited; Twinfinite PRO).

CTSS activity assay. CTSS protease activity was measured using a fluorometric screening kit for CTSS (cat. no. K149, BioVision Inc.) according to the manufacturer's protocol. Fluorescence was measured using the Infinite F200 PRO microplate multi-reader (Tecan Group Limited). The principle relies on the ability of cathepsins to cleave the synthetic 7-amino-4-trifluoromethylcoumarin (AFC)-based peptide substrate to release AFC, which can be measured using a fluorometer. To assess endogenous cellular CTSS activity, MDA-MB-231 cell lysates were analyzed using a CTSS activity assay kit (cat. no. ab65307; Abcam). Cells were collected, frozen, and sonicated using a Branson S-450D Digital Sonifier at 20 kHz in pulse mode (10 sec on/10 sec off for three cycles) on ice before being added to the ice-cold assay buffer supplied with the kit. The enzymatic assay was performed according to the manufacturer's instructions.

GADD45 promoter assay. The GADD45-luciferase (Luc) reporter plasmid was obtained from Addgene, Inc. (cat. no. 8356). 293T cells (American Type Culture Collection) were transfected with 3 μg GADD45-Luc construct using Lipofectamine 2000 (cat. no. 11668019; Invitrogen; Thermo Fisher Scientific, Inc.) according to the manufacturer's protocol. Cells were transfected for 24 h at 37˚C and treated with Peme (0-30 μM) for 12 or 24 h at 37˚C. Luc activity was measured using the Luciferase Assay System kit (cat. no. E4030; Promega Corporation) according to the manufacturer's instructions.

Reverse transcription (RT)PCR. MDA-MB-231 cells were seeded into 60 mm dishes at a density of $3x10^5$ cells/dish in 3 ml RPMI-1640 medium. Total RNA was isolated using QIAzol Lysis Reagent (cat. no. 79306; Qiagen GmbH) according to the manufacturer's instructions. Total RNA (1 μg) was reverse-transcribed into cDNA using the ReverTra Ace qPCR RT master mix with genomic DNA remover (cat. no. FSQ-101; Toyobo Co., Ltd.) according to the manufacturer's protocol. PCR amplification was performed using a standard Taq DNA polymerase (cat. no. P0701-050; GenDEPOT, LLC) and gene-specific primers. The thermocycling conditions were as follows: initial denaturation at 95˚C for 5 min, followed by 28 cycles of denaturation at 95˚C for 30 sec, annealing at 58˚C for 30 sec and extension at 72˚C for 30 sec, followed by a final extension at 72˚C for 5 min. PCR products were separated by agarose gel electrophoresis and visualized using an Image Analyzer (E-graph; ATTO Corp.). GAPDH was used as an internal control. The primer sequences were as follows: BRCA1: Forward, 5'-TTGCGGGAGGAAAATGGGTAG TTA-3' and reverse, 5'-TGTGCCAAGGGTGAATGATGA AAG-3' and GAPDH: Forward, 5'-GTCTCCTCTGACTTC AACAGCG-3' and reverse, 5'-ACCACCCTGTTGCTGTAG CCAA-3'.

Irradiation. For *in vitro* irradiation, MDA-MB-231 and HCC70 cells were seeded at a density of $3x10^5$ cells/dish in 60 mm culture dishes and maintained in RPMI-1640 and DMEM, respectively, at 37˚C until 70-80% confluence. Cells were exposed to 5 or 10 Gy γ-rays at room temperature using a ^{137}Cs γ-ray source (Elan 3000; Atomic Energy of Canada) at a dose rate of 3.81 Gy/min. Cells were returned to the incubator and harvested 12, 24 or 48 h after irradiation. For *in vivo* irradiation, tumor-bearing mice were anesthetized by intraperitoneal administration of 50 mg/kg Zoletil (Virbac) and 10 mg/kg Rompun (Elanco) prior to local irradiation using an X-RAD 320 Biological Irradiator (Precision X-Ray), consistent with previously reported rodent anesthesia protocols (34-37). Irradiation was delivered at a dose of 2 or 4 Gy with a dose rate of ~1 Gy/min at room temperature, and lead shielding was applied to minimize exposure of non-tumor tissue.

Western blotting. Cells were lysed with RIPA buffer [50 mM Tris-HCl (pH 7.5), 150 mM NaCl, 1% NP-40, 0.1% SDS] and 1% sodium deoxycholate supplemented with 1 mM Na_3VO_4, 1 mM dithiothreitol, 1 mM phenyl-methyl-sulfonyl fluoride and protease inhibitor cocktail (cat. no. 539131-10VLCN; Calbiochem; Merck KGaA). Protein concentrations were determined using the Bradford assay. The samples were boiled for 5 min, and 20 μg protein/lane was separated by SDS-PAGE using 6-15% gel. Proteins were transferred onto nitrocellulose membranes, which were blocked with 5% skim milk for 1 h at room temperature. Membranes were incubated with primary antibodies at 4˚C (1:1,000) overnight, followed by incubation with HRP-conjugated anti-mouse (1:3,000; cat. no. SA001-500; GenDEPOT) or HRP-conjugated anti-rabbit IgG (1:3,000; cat. no. SA002-500; GenDEPOT) for 1 h at room temperature. Protein bands were visualized using FEMTO-ECL (cat. no. DG-WT-200; Dogen) and a chemiluminescence imaging system (GBOX CHEMI XX9; Syngene Europe). Band intensities were quantified using ImageJ software (version 1.45; National Institutes of Health), with β-actin used as the loading control.

Cell fractionation. Subcellular fractionation was performed using a Subcellular Protein Fractionation kit (cat. no. 78840; Thermo Fisher Scientific, Inc.) according to the manufacturer's instructions. Briefly, harvested cell pellets obtained by centrifugation at 500 x g for 5 min at 4˚C were resuspended in

cytoplasmic extraction buffer and incubated at 4˚C for 10 min with gentle mixing, followed by centrifugation at 500 x g for 5 min at 4˚C to collect the cytoplasmic fraction. The pellets were resuspended in nuclear extraction buffer, incubated at 4˚C for 30 min with intermittent mixing and centrifuged at 5,000 x g for 5 min at 4˚C to obtain the nuclear fraction. The purity of each fraction was verified by immunoblotting using β-actin as a cytosolic marker and lamin A/C as a nuclear marker as aforementioned.

Immunofluorescence staining. MDA-MB-231 cells were seeded at a density of $4x10^4$ cells/coverslip on glass coverslips and treated with Peme (5, 10 or 30 μM) for 24 h at 37˚C. Cells were fixed with 4% paraformaldehyde (PFA) for 10 min at room temperature, permeabilized with 0.1% Triton X-100 and blocked with 5% bovine serum albumin (cat. no. A0100-010; GeneDEPOT) for 1 h at room temperature. Cells were incubated with anti-BRCA1 primary antibody (1:200; cat. no. SC-6954; Santa Cruz Biotechnology, Inc.) overnight at 4˚C, followed by Alexa Fluor-conjugated secondary antibody (1:500; cat. no. A-11004; Invitrogen; Thermo Fisher Scientific, Inc.) for 1 h at room temperature. Nuclei were counterstained and mounted using a DAPI-containing mounting medium (cat. no. F6057; Sigma-Aldrich; Merck KGaA). Images were acquired using a fluorescence microscope (Zeiss). BRCA1 fluorescence intensity was quantified using ImageJ (version 1.54p; National Institutes of Health) from ≥3 independent experiments.

Cycloheximide (CHX) chase assay. The stability of BRCA1 protein was evaluated using a CHX (cat. no. C4859; Sigma-Aldrich; Merck KGaA) chase assay. MDA-MB-231 cells were treated with CHX (100 μg/ml) in the presence or absence of Peme (10 μM) for 0-24 h at 37˚C. Cells were harvested and lysed in RIPA buffer, and 30 μg proteins/lane was analyzed by SDS-PAGE as aforementioned.

Nickel pull-down assay. Nickel pull-down assays were performed to detect ubiquitinated BRCA1. Cells were pretreated with MG132 (10 μM) for 6 h at 37˚C to inhibit proteasomal degradation prior to harvest. Cells were lysed in urea lysis buffer containing 8 M urea, 100 mM Na_2HPO_4, 10 mM Tris-HCl (pH 8.0), 10 mM imidazole and 0.2% Triton X-100 and lysates were fully disrupted by ultrasonication at 20 kHz in pulse mode (10 sec on/10 sec off for three cycles) on ice. The clarified lysates were incubated with Ni-NTA Agarose beads (cat. no. 30210; Qiagen GmbH) for 4 h at 4˚C with gentle rotation to capture His-tagged proteins. Beads were washed with wash buffer and eluted with 2X SDS loading buffer. The eluted proteins were analyzed by immunoblotting using the target antibodies to assess ubiquitination as aforementioned.

Docking study. A structure-based virtual screening of FDA-approved drugs from the ZINC database (zinc.docking.org/) was performed to identify potential CTSS inhibitors. Molecular docking simulations were performed using the Maestro software package (version 2022-4; Schrödinger, LLC). The crystal structure of the BRCA1 BRCT domain (Protein Data Bank ID: 3K0H) was imported into Maestro and prepared using the Protein Preparation Wizard (Schrödinger Release 2022-4; Schrödinger, LLC). Ligand structures (Peme, compound 15, Bractoppin and the minimal phospho-tetrapeptide) were prepared using the LigPrep module (Schrödinger Release 2022-4; Schrödinger, LLC) with default settings, generating low-energy conformers and appropriate protonation states at pH 7.0±0.5. The receptor grid was generated around the phosphopeptide-binding site, defined by the co-crystallized ligand coordinates. To validate the docking protocol, the original co-crystallized ligand was re-docked into the binding site, and the root-mean-square deviation (RMSD) relative to the experimental pose was calculated. Binding poses were analyzed in Maestro and key molecular interactions such as hydrogen bonds, aromatic-hydrogen bonds and salt bridges were annotated.

Flow cytometry. Cells were cultured, harvested, washed twice with PBS. Cells were incubated in the dark for 10 min at 37˚C in PBS containing 10 μg/ml propidium iodide (PI; cat. no. P4170; Sigma-Aldrich). Flow cytometric analysis was performed using a FACSCalibur flow cytometer (version 3.0; Becton Dickinson Biosciences). Data were analyzed using CellQuest Pro software (version 5.2; Becton Dickinson Biosciences).

Clonogenic survival assay. For clonogenic assays, MDA-MB-231 cells were seeded in 6 well plates at low density (200-1,000 cells/well) and allowed to adhere overnight. Cells were then treated with Peme (1 or 2 μM) at 37˚C and/or IR (0.5 Gy). After 24 h Peme treatment, the medium was replaced with drug-free medium, and cells were incubated for 10-14 days at 37˚C to allow colony formation. Colonies were fixed with 4% PFA for 15 min and stained with 0.5% crystal violet (cat. no. C0775; Sigma-Aldrich), both at room temperature. Colonies containing >50 cells were counted manually using ImageJ software (version 1.54p; National Institutes of Health). The surviving fraction was calculated relative to the non-irradiated control group and expressed as the mean ± SD from three independent experiments.

Tumor xenograft experiment using non-obese diabetic/severe combined immunodeficiency (NOD-SCID) mice. All animal studies were conducted in accordance with the Institutional Animal Care and Use Committee (IACUC) guidelines and were approved by the IACUC of Ewha Womans University, Seoul, Republic of Korea (approval no. EWHA IACUC 23-049-t). Mice were housed under specific-pathogen-free conditions at 22±2˚C and 50±10% relative humidity under a 12 h light/12 h dark cycle, with a standard diet and water provided *ad libitum*. For tumor xenograft experiments, MDA-MB-231 cells ($5x10^6$ cells in 100 μl PBS) were subcutaneously injected into the right thigh (hindlimb) of 5-week-old female NOD-SCID mice weighing ~18 g, obtained from Koatech (Pyeongtaek, Republic of Korea). A total of 36 mice were used, with four or five mice per group. Tumor growth was monitored 2-3 times per week beginning 2 weeks after MDA-MB-231 cell injection. When tumors reached a mean volume of ~200 mm^3, mice were randomly divided into four groups: i) Control (vehicle only), ii) Peme (100 mg/kg, intraperitoneal injection, once/week), iii) IR-control and iv) IR + Peme (100 mg/kg, once/week). The 4 Gy experiment was terminated on day 40, whereas the 2 Gy experiment was terminated on day 35. The maximum tumor

Table I. FDA-approved drugs based on *in silico* high-throughput screening.

ZINC ID	Geom rank	Geom total score	GeomX Rank	GeomX Total score	Drug	Indications
ZINC150338755	1	11.3040	1	12.7377	Venetoclax	Oral anticancer drug (Bcl-2 inhibitor)
ZINC145401681	2	10.8922	2	10.8467	Sofosbuvir	Hepatitis C (NS5B protein inhibitor)
ZINC34636383	3	9.8709	36	8.4490	Olodaterol	COPD (β2 receptor agonist)
ZINC3806063	4	9.7957	4	9.8212	Silodosin	Benign prostatic hyperplasia (α1 antagonist)
ZINC4074875	7	9.5762	10	9.6527	Candesartan	Hypertension (angiotensin II receptor inhibitor)
ZINC1540998	8	9.5306	8	9.6813	Pemetrexed	Anticancer drug (GARFT inhibitor)
ZINC49933061	9	9.5233	14	9.3968	Dronedarone	Cardiac arrhythmia (sodium channel blocker)
ZINC38945666	10	9.5167	19	9.1479	Sodium phenylbutyrate	Inborn urea cycle disorder
ZINC3806104	36	8.0395	5	9.8140	Tirofiban	Antiplatelet drug
ZINC4474405	25	8.4884	11	9.5393	Bimatoprost	Glaucoma (PGF2α analog)

NS5B, non-structural protein 5B; COPD, chronic obstructive pulmonary disease; GARFT, glycinamide ribonucleotide formyltransferase; PGF, prostaglandin F; Geom, Surflex-Dock Geom mode; GeomX, Surflex-Dock GeomX mode.

diameter was not permitted to exceed 20 mm. No animals required early euthanasia because of this endpoint. Mice were euthanized by gradual-fill CO_2 inhalation at a volume displacement rate of 30% of the chamber volume/min, in accordance with the approved institutional animal protocol (38,39). Death was confirmed by cessation of respiration and heartbeat with the absence of reflexes. Tumor volume was calculated as (length/2) x (width^2). For the 4 Gy experiment, only the tumor volume data were retained; therefore, the single largest tumor diameter could not be retrospectively determined with confidence.

Tumor growth inhibition (TGI). TGI was calculated to evaluate the antitumor efficacy of Peme alone or in combination with IR. TGI (%) was calculated as: TGI (%)=[1-(mean tumor volume of treated group/mean tumor volume of control group)] x100. A TGI value of 100% indicated complete tumor growth suppression, whereas a value of 0% indicates no inhibitory effect compared with the control. Data are presented as the mean ± SEM from ≥3 independent experiments.

Immunohistochemical staining. Tumor tissue was fixed in 10% neutral-buffered formalin for 24 h at room temperature, embedded in paraffin and sectioned at 4 μm thickness. Sections were deparaffinized in xylene and rehydrated through graded ethanol. Antigen retrieval was performed in 10 mM citrate buffer (pH 6.0) for 20 min. Endogenous peroxidase activity was blocked with 3% hydrogen peroxide for 10 min at room temperature. Sections were then blocked with serum supplied with the VECTASTAIN Elite ABC-HRP kit (Vector Laboratories) for 20 min at room temperature. Sections were incubated overnight at 4˚C with primary antibodies against Ki-67 (cat. no. M7240; Dako; Agilent Technologies, Inc.), BRCA1 (cat. no. SC-6954; Santa Cruz Biotechnology, Inc.) and γ-H2AX (all 1:200; cat. no. 5438; Cell Signaling Technology, Inc.). Secondary antibody detection was performed using the VECTASTAIN Elite ABC-horseradish peroxidase kit for mouse (cat. no. PK-6102; Vector Laboratories) or rabbit IgG (cat. no. PK-6101; Vector Laboratories), with the biotinylated secondary antibodies diluted 1:200 according to the manufacturer's protocol. Immunoreactivity was visualized using DAB (cat. no. 54-10-00; SeraCare) and counterstained with hematoxylin for 1 min at room temperature. Images were acquired using a Carl Zeiss Axio Scope light microscope (Zeiss). Staining intensity was quantified using ImageJ software (version 1.54p; National Institutes of Health).

Statistical analysis. All data are presented as the mean ± SD or SEM of at least three independent experiments, and were analyzed using GraphPad Prism 9 (GraphPad Software Inc.; Dotmatics). Statistical significance was determined by one- or two-way ANOVA followed by Dunnett's multiple comparisons test, Tukey's post hoc test, or an unpaired Student's t-test. $P<0.05$ was considered to indicate a statistically significant difference.

Results

Peme enhances BRCA1 protein expression independently of CTSS inhibition. Inhibition of CTSS has been proposed as a strategy to stabilize BRCA1 protein levels (12,14,23). To identify potential CTSS inhibitors among clinically available compounds, the present study conducted a structure-based virtual screening of Food and Drug Administration-approved drugs from ZINC database, which yielded 10 candidate molecules (Table I). When these candidates were evaluated for their effects on BRCA1 protein levels by immunoblotting, Peme produced the greatest increase in BRCA1 expression among the tested compounds. E-64, a pan-CTSS inhibitor, was used as a positive control (Fig. 1A). To determine whether

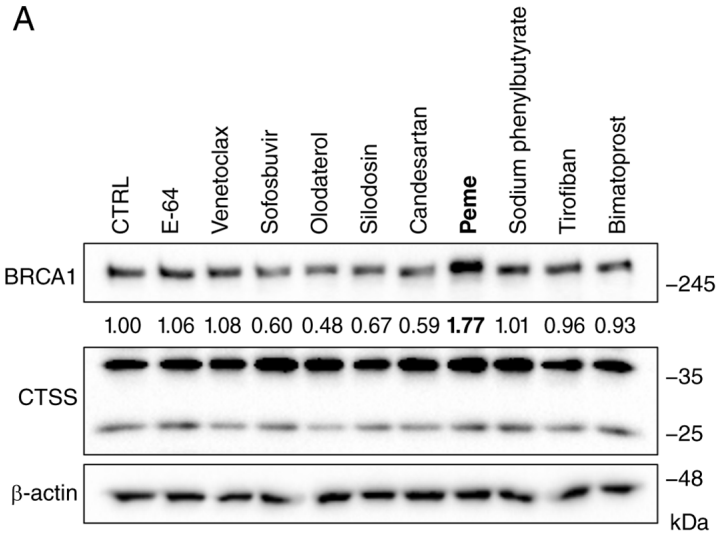

B

Compound	IC_{50} (μM)
RO5461111	0.014 ± 0.00
Z-FL-COCHO	15.930 ± 7.13
Candesartan	398.140 ± 31.29
Peme	546.122 ± 115.09

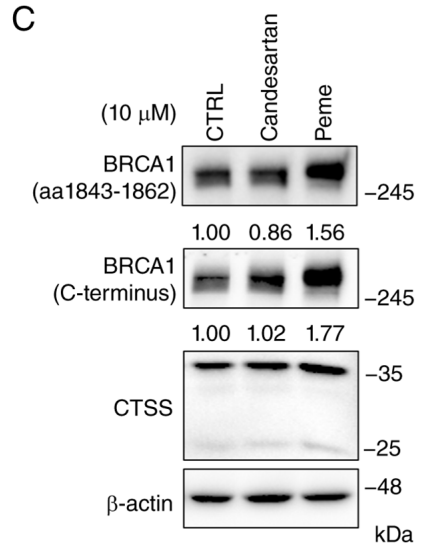

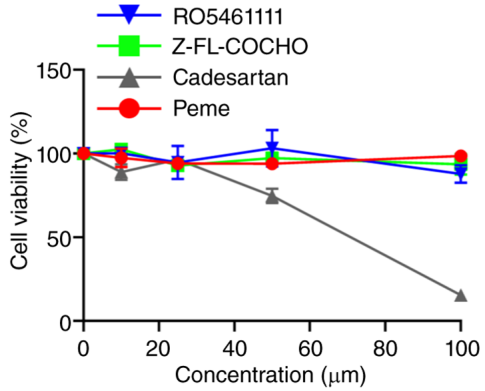

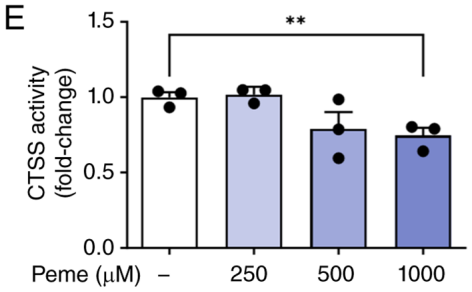

Figure 1. Peme enhances BRCA1 protein expression independently of CTSS inhibition. (A) Immunoblot analysis of BRCA1 and CTSS in MDA-MB-231 cells treated for 24 h with the indicated screened compounds; E-64 was included as a positive control. β-actin was used as a loading control. Numbers indicate the relative BRCA1 band density normalized to β-actin. (B) IC_{50} values for CTSS inhibitors were determined using CTSS enzymatic activity assay. (C) Immunoblot analysis of BRCA1 protein levels in MDA-MB-231 cells treated with candesartan or Peme. (D) Cell viability assay. (E) CTSS enzymatic activity in MDA-MB-231 cells was determined following treatment with Peme (0-1,000 μM) for 24 h. **P<0.01. Peme, pemetrexed; CTSS, cathepsin S; IC_{50}, half-maximal inhibitory concentration; CTRL, control; aa, amino acid.

this effect was CTSS-dependent, CTSS enzymatic assay was performed. Peme exhibited a weak inhibitory effect, with a half-maximal inhibitory concentration (IC_{50}) of 546.122 μM, whereas RO (40) and ZFL (41) exhibited IC_{50} values of 0.014 and 15.930 μM, respectively (Fig. 1B). Although candesartan demonstrated stronger CTSS inhibition than Peme, it did not induce BRCA1 expression (Fig. 1A and C) but showed greater cytotoxicity than Peme (Fig. 1D). Therefore, it was excluded from further analysis. In MDA-MB-231 TNBC cells, Peme (1,000 μM) induced a significant decrease in CTSS enzymatic activity compared with the control (Fig. 1E). Collectively, these findings indicated that, unlike RO and ZFL, Peme-mediated BRCA1 upregulation occurred independently of CTSS inhibition. Peme, RO and ZFL did not

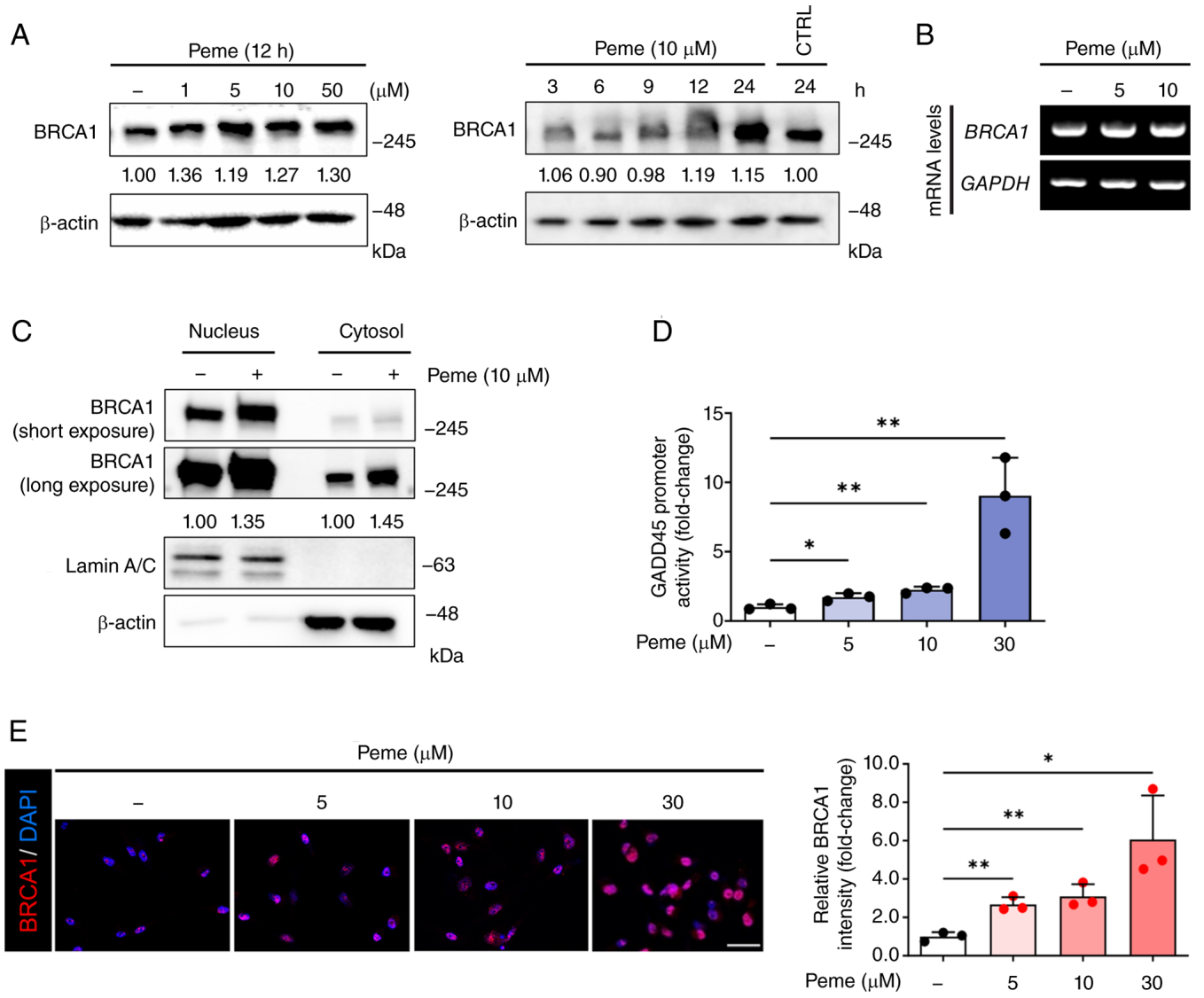

Figure 2. Peme upregulates BRCA1 at the post-transcriptional level and promotes its cytosolic accumulation. (A) Dose- and time-dependent regulation of BRCA1 expression by Peme in MDA-MB-231 cells. Numbers indicate the relative BRCA1 band density normalized to β-actin. (B) PCR analysis of BRCA1 mRNA levels following Peme treatment. (C) Cell fractionation showing nuclear accumulation of BRCA1 following 10 μM Peme treatment for 24 h. Lamin A/C and β-actin were used as nuclear and cytosolic markers, respectively. (D) GADD45 promoter luc assay showing dose-dependent activation by Peme in 293T cells. Cells were transfected with a GADD45-luc reporter and treated with Peme for 24 h. Luciferase activity is presented as fold induction relative to control. (E) Representative immunofluorescence of BRCA1 expression following Peme treatment. Cells were treated with Peme for 24 h and stained for BRCA1 (red) and nuclei (DAPI, blue). Scale bar, 200 μm. *P<0.05, **P<0.01. Peme, pemetrexed; luc, luciferase; CTRL, control; GADD45, growth arrest and DNA damage-inducible 45.

display significant cytotoxicity (Fig. 1D). Peme increased BRCA1 protein levels in a dose- and time-dependent manner, with maximal induction observed at 12 h at all concentrations (Fig. 2A). Notably, BRCA1 mRNA expression remained unchanged following Peme treatment (Fig. 2B), indicating a post-translational regulatory mechanism. The pro-apoptotic function of BRCA1 is regulated by its cytosolic part (23,42). Consistent with this, cell fractionation experiments revealed that Peme enhanced BRCA1 protein levels in both the nuclear and cytosolic compartments (Fig. 2C). Functionally, Peme increased GADD45 promoter activity, a downstream target of BRCA1, supporting the upregulation of functionally active BRCA1 (Fig. 2D). Immunofluorescence analysis confirmed a dose-dependent increase in BRCA1 fluorescence intensity 24 h after Peme exposure (Fig. 2E).

Peme inhibits proteasomal degradation of BRCA1 protein. Peme increased BRCA1 protein expression at concentrations lower than those required for CTSS inhibition in MDA-MB-231 cells, suggesting that its effect involved mechanisms beyond CTSS suppression. Because BRCA1 mRNA levels were not altered by Peme, the present study examined whether the increase in BRCA1 protein expression was mediated by enhanced protein stability. CHX chase analysis showed that Peme significantly prolonged BRCA1 protein stability (Fig. 3A). As BRCA1 undergoes degradation via the ubiquitin-proteasome pathway (14), the present study examined whether Peme interferes with this process. Treatment with MG132, a proteasome inhibitor, increased BRCA1 protein levels and Peme further delayed BRCA1 degradation, suggesting that Peme suppressed the

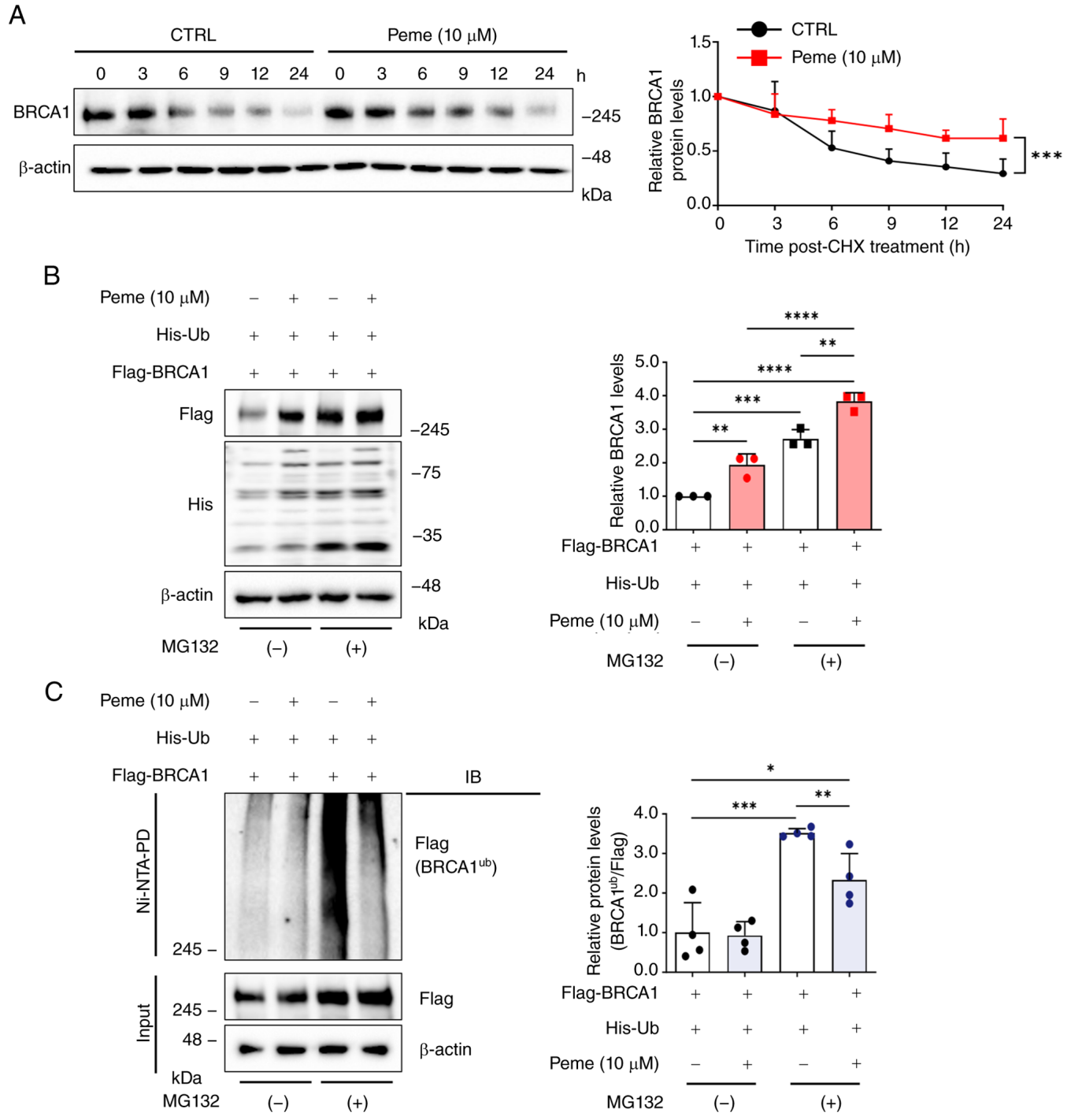

Figure 3. Peme stabilizes BRCA1 protein by inhibiting Ub-proteasome-mediated degradation. (A) MDA-MB-231 cells were treated with 10 μM Peme or vehicle followed by CHX (100 μg/ml). BRCA1 protein levels were analyzed and the relative band density was quantified to determine protein stability. (B) 293T cells were treated with the proteasome inhibitor MG132 in the presence or absence of Peme. Immunoblot analysis showed MG132 treatment increased BRCA1 protein levels, and co-treatment with Peme further enhanced and prolonged BRCA1 stabilization. (C) 293T cells expressing His-Ub and Flag-BRCA1 were treated with Peme (10 μM) and/or MG132 (10 μM) for 6 h. Ubiquitinated BRCA1 was isolated by His pull-down and detected by immunoblotting with the anti-Flag antibody. *P<0.05, **P<0.01, ***P<0.001, ****P<0.0001. Peme, pemetrexed; CHX, cycloheximide; His, histidine tag; CTRL, control; NTA, nitrilotriacetic acid; PD, pull-down; Ub, ubiquitin.

ubiquitin-proteasome-mediated degradation of BRCA1 (Fig. 3B). Consistently, nickel pull-down assays using His-tagged ubiquitin showed that the MG132-induced increase in BRCA1 ubiquitination was attenuated by concurrent Peme treatment (Fig. 3C). This highlighted the ability of Peme to hinder ubiquitin-mediated degradation of BRCA1. To identify the domain responsible for Peme-mediated stabilization, BRCA1 deletion constructs lacking either the RING or BRCT domain were generated. Peme failed to increase BRCA1 protein expression in cells expressing the BRCT-deleted (ΔBRCT) construct, whereas cells expressing the RING-deleted (ΔRING) construct retained Peme responsiveness (Fig. 4A). Peme-induced GADD45 promoter activation was abolished in ΔBRCT-expressing cells but

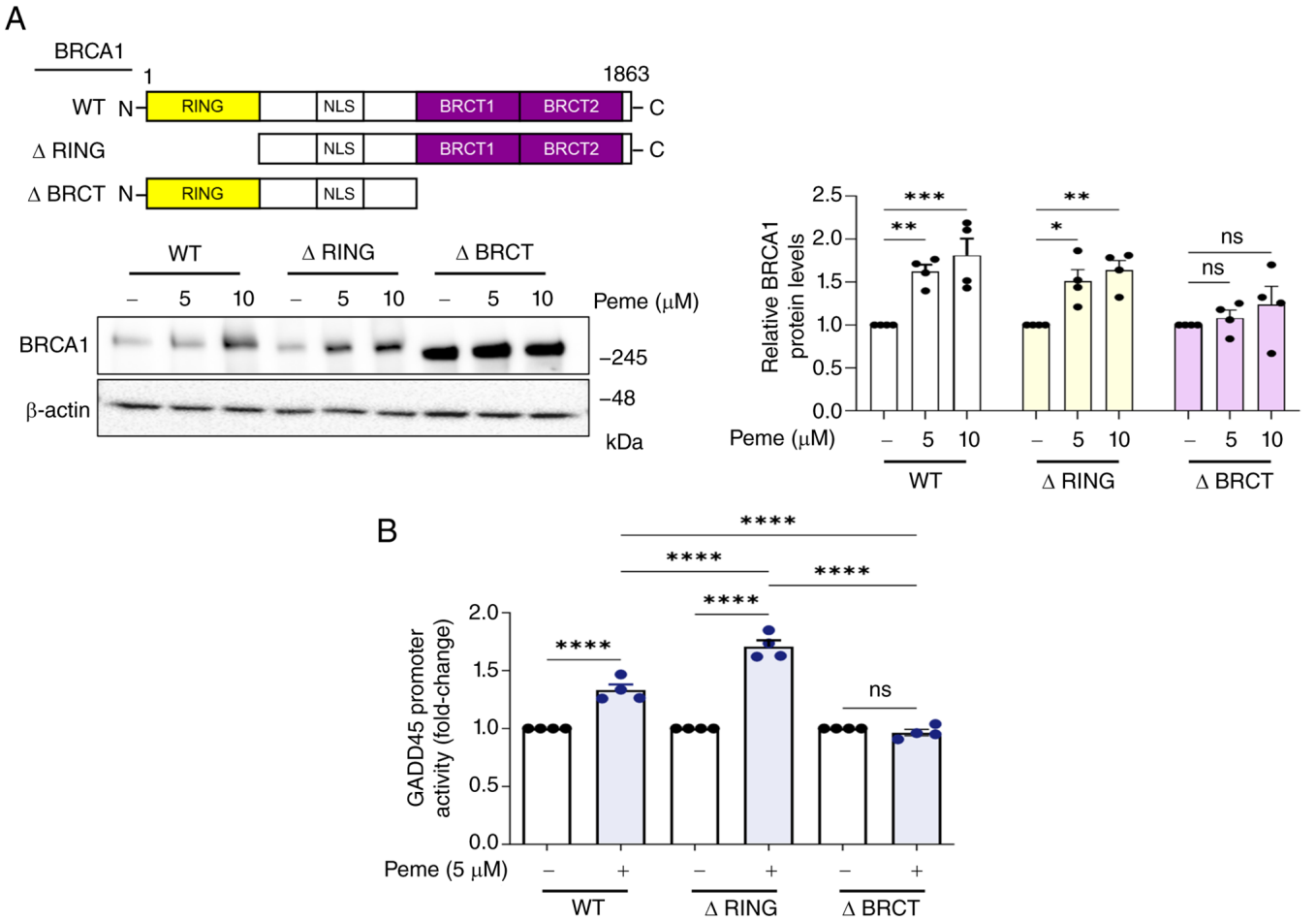

Figure 4. BRCT domain is required for Peme-mediated BRCA1 stabilization and downstream signaling. (A) Schematic representation of BRCA1 deletion mutants (ΔRING and ΔBRCT). 293T cells were transfected with WT or mutant BRCA1 constructs and treated with Peme (0-10 μM) for 12 h. BRCA1 protein expression was determined by immunoblotting. (B) GADD45 promoter luc assay showing BRCA1 domain-dependent activation by Peme in 293T cells. Cells expressing WT, ΔRING or ΔBRCT BRCA1 constructs were transfected with a GADD45-luc reporter and treated with 5 μM Peme for 12 h. Luc activity is presented as fold induction relative to control. *P<0.05, **P<0.01, ***P<0.001, ****P<0.0001. BRCT, BRCA1 C-terminal; Peme, pemetrexed; RING, really interesting new gene; WT, wild-type; GADD45, growth arrest and DNA damage-inducible 45; luc, luciferase; ns, not significant.

preserved in ΔRING-expressing cells (Fig. 4B). Together, these findings demonstrated that Peme enhanced BRCA1 stability by suppressing its ubiquitin-proteasome-mediated degradation in a BRCT domain-dependent manner.

To investigate the interaction between Peme and the BRCT domain, molecular docking analysis was performed. The docking protocol was validated by re-docking the original co-crystallized ligand into the binding site, which yielded an RMSD of 1.427 Å relative to the experimental pose, confirming the reliability of the docking protocol (Fig. 5A). Based on the BRCA1 structure co-crystallized with a phospho-tetrapeptide ligand, Peme was predicted to bind the same region with a similar binding pose (Fig. 5A). Peme was well accommodated within the BRCT binding pocket, engaging the minimal tetrapeptide recognition sequence. The docking score of Peme (-5.801) was comparable with that of the phospho-tetrapeptide (-6.145). The predicted binding pose indicated that Peme formed hydrogen bond interactions with Ser1655 and Asn1774, similar to the tetrapeptide, and extended toward the C-terminal BRCT domain by interacting with Asp1813 (Fig. 5B). Previously reported BRCT-binding small molecules, including compound 15 (43) and Bractoppin (44), were also analyzed. The docking score of Peme was similar to or better than the docking scores of the reference compounds (Fig. 5C). Collectively, these findings suggested that the BRCT domain may be involved in the stabilizing effect of Peme on BRCA1.

Peme triggers cell death in a BRCA1-dependent manner. Mechanistically, Peme induced BRCA1 upregulation in a dose- and time-dependent manner, accompanied by increased PARP1 cleavage, with maximal induction observed at 10 μM after 24 h (Fig. 6A). These findings indicated that Peme induced apoptosis. To determine whether Peme-induced cell death depends on BRCA1 expression, cells were transfected with BRCA1-specific siRNA. BRCA1 silencing markedly attenuated Peme-induced apoptotic events, including PARP1 and caspase-3 cleavage, which are established markers of apoptosis (45,46) (Fig. 6B). Consistent results were obtained from flow cytometric analysis of PI-stained cells, showing a significant decrease in Peme-induced cell death following BRCA1 knockdown (Fig. 6C). Collectively, these results demonstrated that Peme triggers apoptosis in a BRCA1-dependent manner.

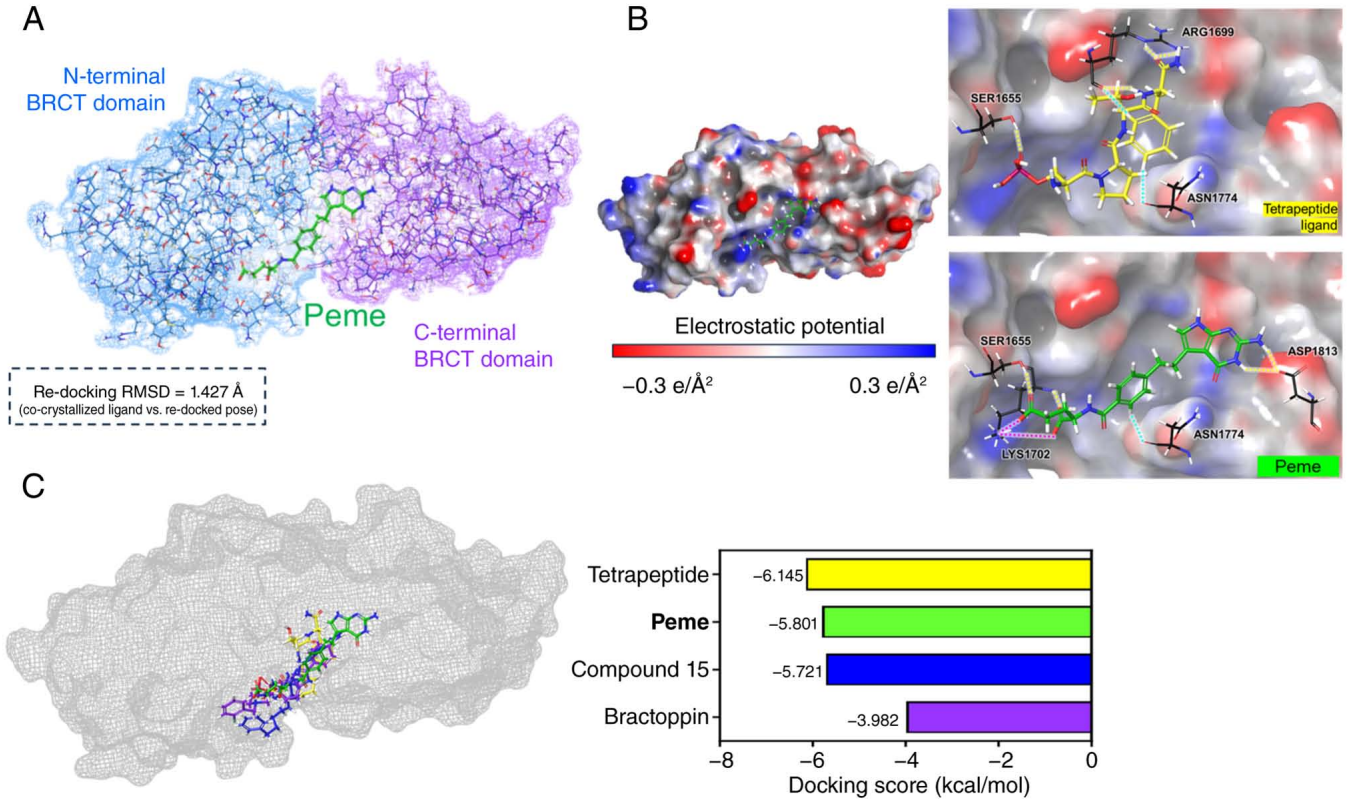

Figure 5. Peme occupies the phosphopeptide-binding pocket of the BRCA1 BRCT domain. (A) Predicted binding pose of Peme in the BRCT domain of BRCA1 (Protein Data Bank ID: 3K0H). The re-docking RMSD of the co-crystallized ligand relative to the experimental pose was 1.427 Å. (B) Comparison of interacting residues between the co-crystallized phosphopeptide (yellow) and Peme (green). The surface of the BRCT domain is colored according to electrostatic potential. Pink dash, salt bridge; cyan dash, aromatic hydrogen bond; yellow dash, hydrogen bond. (C) Docking scores for the minimal tetrapeptide, Peme, Compound 15, and Bractoppin. The minimal tetrapeptide (yellow), Peme (green), compound 15 (blue) and Bractoppin (purple) were individually docked into the BRCT domain structure. Compound 15 and Bractoppin were included based on previously reported BRCT-binding compounds (43,44). Docking scores are presented in kcal/mol. Peme, pemetrexed; BRCT, BRCA1 C-terminal; RMSD, root-mean-square deviation.

Peme makes TNBC cells more responsive to irradiation. BRCA1 suppresses tumor growth by promoting apoptosis and maintaining genomic stability in cancer cells (47,48). Based on this, it was hypothesized that combining Peme with IR may augment apoptosis and thereby potentiate the cell response to irradiation in TNBC cells. In MDA-MB-231 cells, BRCA1 protein levels increased progressively following Peme treatment; this induction was further enhanced by IR co-treatment (Fig. 7A). Consistently, GADD45 promoter activity, a downstream indicator of BRCA1 pathway activation (49), was significantly potentiated by combined Peme and IR treatment (Fig. 7B). Furthermore, markers of apoptosis, including cleaved PARP1, were more prominently induced by the combination treatment (Fig. 7C). This was further supported by the similar induction of BRCA1, cleaved PARP, cleaved caspase-3 and caspase-3 in HCC70 cells, another TNBC cell line (Fig. S1A). These molecular changes corresponded with increased cell death and decreased colony-forming ability (Fig. 7D and E). Preliminary clonogenic assays using 1 Gy irradiation showed that IR alone markedly decreased colony formation, supporting the use of a lower IR dose in the main clonogenic assay (Fig. S1B). BRCA1 knockdown using siRNA markedly diminished the induction of cleaved caspase-3 under combined Peme and IR exposure (Fig. 7F). This observation supported the hypothesis that the enhanced effect of combined Peme and IR treatment was, at least in part, BRCA1-dependent.

Radiosensitization by Peme in a TNBC cell xenograft mouse model. To confirm whether the *in vitro* effects of Peme, including BRCA1 induction and enhanced radiosensitivity, could be reproduced *in vivo*, a tumor xenograft model was established using MDA-MB-231 TNBC cells. When tumors reached ~200 mm^3, mice were exposed to IR (2 or 4 Gy), followed by intraperitoneal administration of Peme (100 mg/kg; Fig. 8A). Peme was administered for 35 or 40 days while monitoring tumor growth. Compared with IR alone, the combination of Peme and IR significantly delayed tumor growth, demonstrating the radiosensitizing potential of Peme, although the overall magnitude of tumor suppression was moderate. The single largest tumor volume was 1,878.68 mm^3 for 4 Gy and 1,787.82 mm^3 for 2 Gy experiment. Although co-administration of Peme with either 2 or 4 Gy for 35 or 40 days did not significantly alter the radiosensitizing effect of Peme, TGI analysis confirmed that the combination of Peme and IR yielded greater tumor suppression than IR alone (Fig. 8B and C). Immunohistochemical analysis of tumor tissue revealed that combined treatment markedly decreased the expression of the proliferation marker Ki-67, while increasing the levels of BRCA1 compared with the corresponding IR-alone groups (Fig. 9A and B). Collectively, these results confirmed that Peme enhanced radiosensitivity *in vivo*, consistent with its BRCA1-dependent mechanism *in vitro*. Peme did not affect overall animal viability or general health throughout the experimental period.

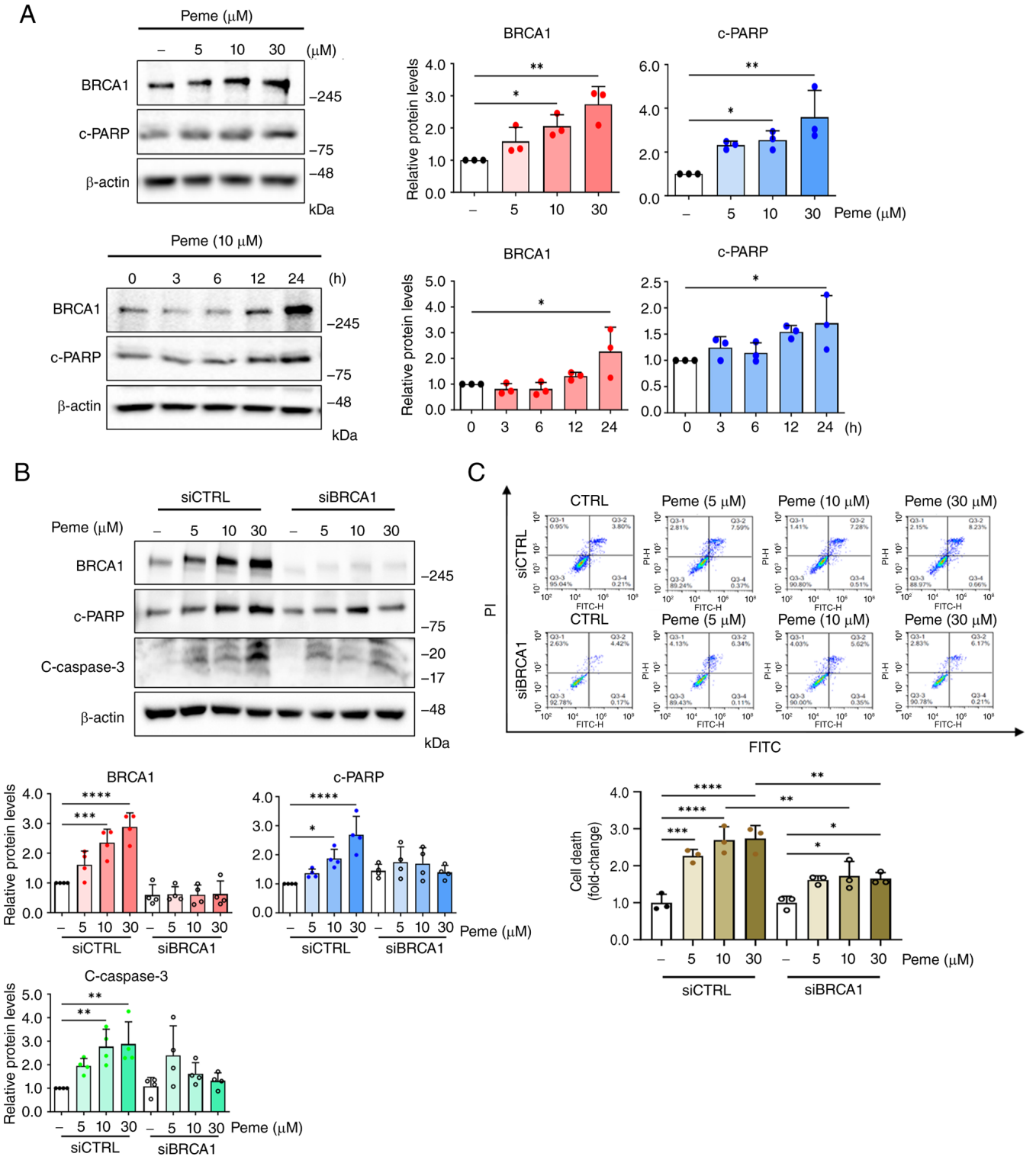

Figure 6. Peme induces BRCA1-dependent death in triple-negative breast cancer cells. (A) MDA-MB-231 cells were treated with Peme. Protein levels of BRCA1 and c-PARP were analyzed by immunoblotting. (B) MDA-MB-231 cells transfected with siCTRL or siBRCA1 were treated with Peme for 24 h. Immunoblot analysis was performed for BRCA1, c-PARP and c-caspase-3. β-actin was used as a loading control. (C) Flow cytometry analysis of PI-stained MDA-MB-231 cells showing Peme-induced cell death in a BRCA1-dependent manner. *P<0.05, **P<0.01, ***P<0.001, ****P<0.0001. Peme, pemetrexed; si, small interfering; CTRL, control; c-, cleaved.

Discussion

TNBC is one of the most aggressive BC subtypes, characterized by the absence of hormone receptors and HER2 amplification, leading to poor prognosis and limited treatment options (50,51). Although the advent of PARP inhibitors such as olaparib represents a therapeutic breakthrough for BRCA1/2 mutant BC, this approach is only effective in a subset of patients with TNBC harboring germline or somatic BRCA1 mutations (52,53). By contrast, most TNBC cases retain wild-type BRCA1 but

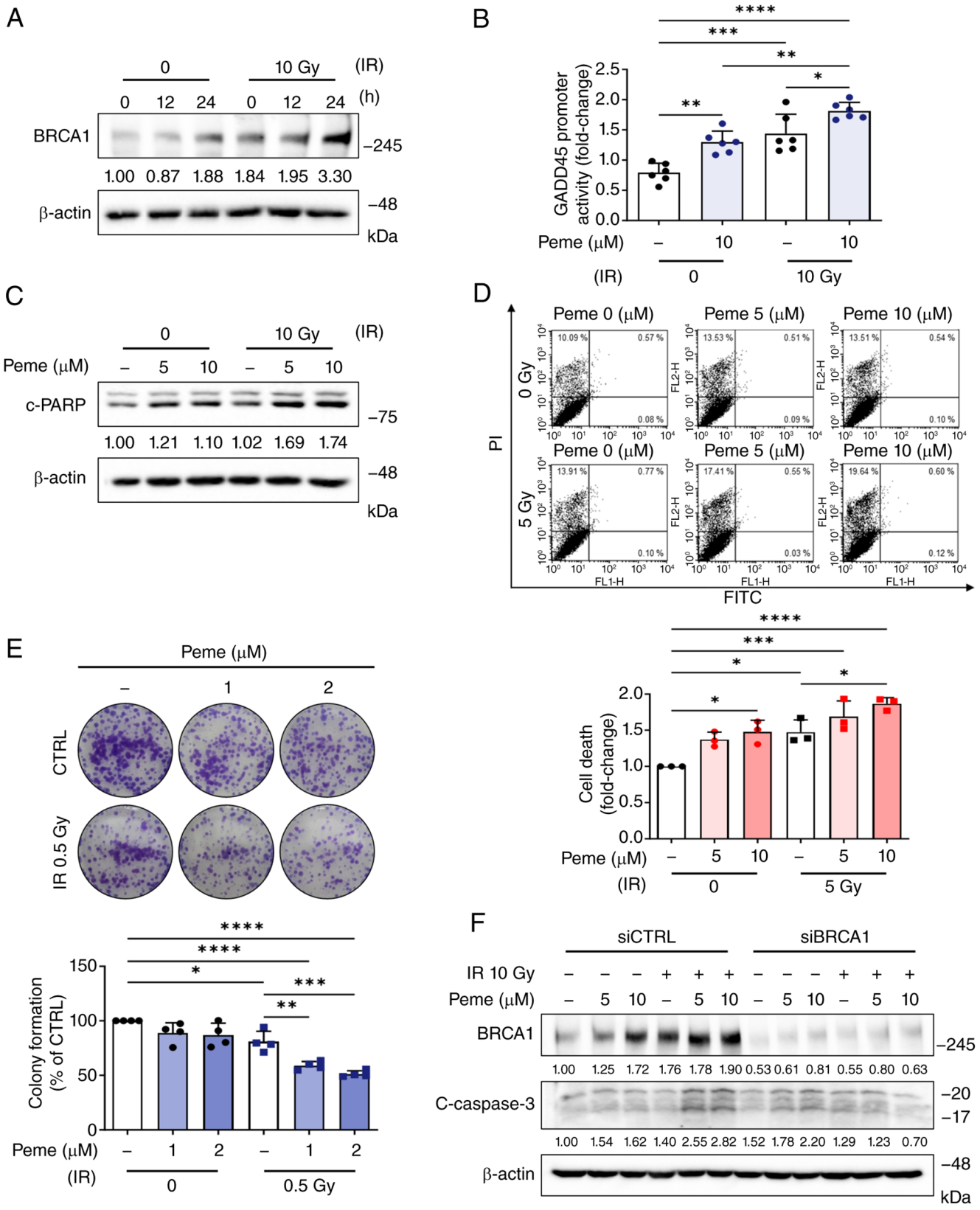

Figure 7. Peme induces radiosensitization in triple-negative breast cancer cells via BRCA1-dependent apoptosis. (A) MDA-MB-231 cells were treated with 10 μM Peme, followed by 10 Gy IR. BRCA1 protein levels were analyzed by immunoblotting. (B) GADD45 promoter luc assay showing activation by combined Peme and IR treatment in 293T cells. Luc activity is presented as fold induction relative to control. (C) Immunoblot analysis was performed for c-PARP. (D) Flow cytometry analysis of PI-stained MDA-MB-231 cells showing that Peme and IR increased cell death. Cells were treated with Peme (0-10 μM) and/or IR (5 Gy) for 24 h and PI-positive cells were quantified as fold change relative to control. (E) Clonogenic survival assay showing decreased colony formation following combined Peme and IR treatment. Colony numbers were normalized to control. (F) BRCA1 knockdown attenuated Peme- and IR-induced apoptosis. MDA-MB-231 cells transfected with siCTRL or siBRCA1 were treated with Peme (0-10 μM) and IR (10 Gy) for 24 h. Immunoblot analysis for BRCA1 and c-caspase-3 was performed with β-actin as a loading control. Relative protein band density is indicated below each lane. *P<0.05, **P<0.01, ***P<0.001, ****P<0.0001. Peme, pemetrexed; IR, ionizing radiation; GADD45, growth arrest and DNA damage-inducible 45; luc, luciferase; c-, cleaved; CTRL, control; si, small interfering.

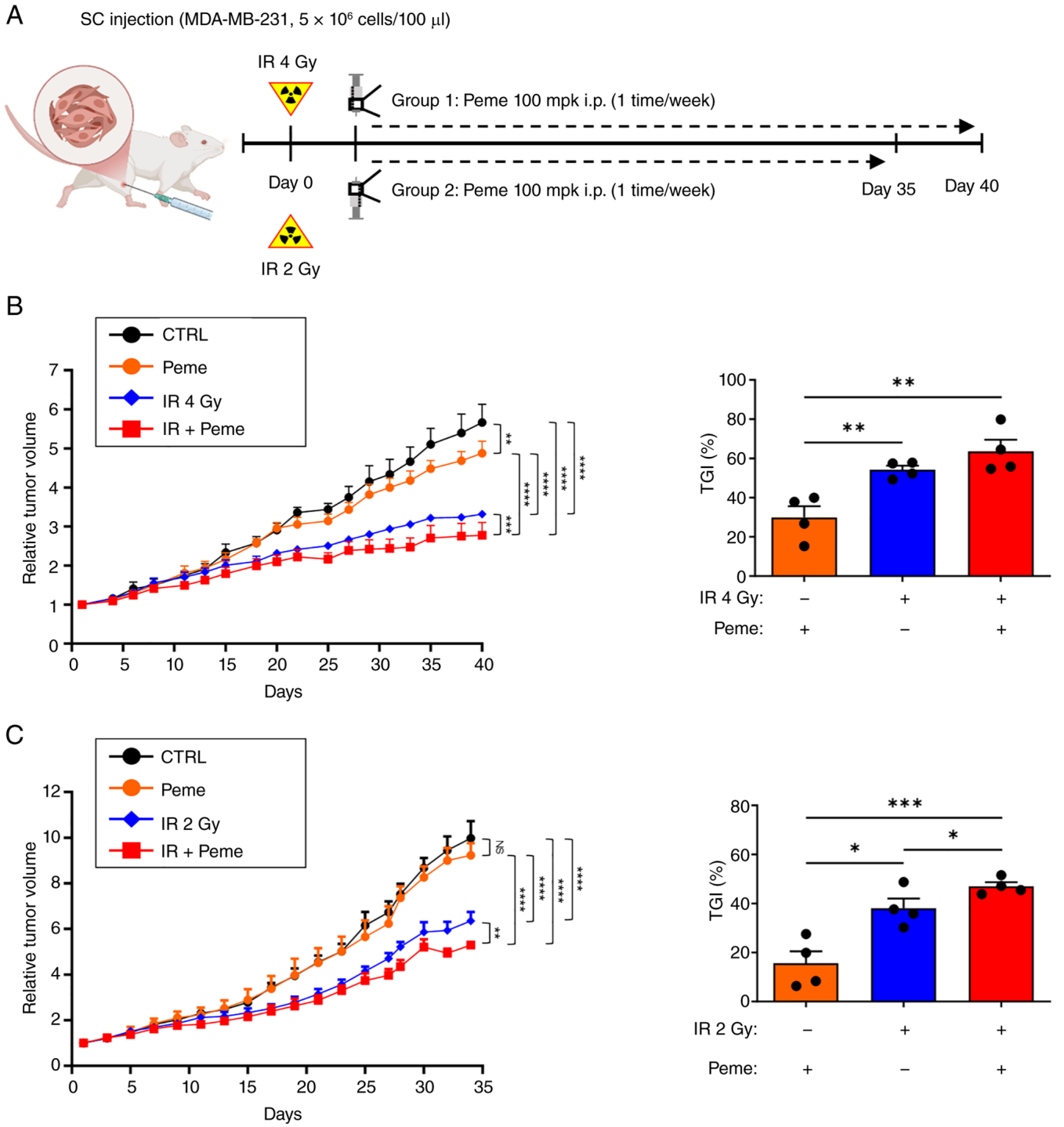

Figure 8. Peme enhances the antitumor effect of irradiation in TNBC xenografts. (A) Schematic of the *in vivo* experimental design. MDA-MB-231 cells were SC injected into the hind legs of NOD/SCID mice to establish TNBC xenografts. When tumors reached ~200 mm^3, mice were treated with Peme (100 mg/kg, i.p., once/week) and/or IR (2 or 4 Gy). Tumor growth was monitored for 35 and 40 days, respectively. (B) Tumor growth curves of xenograft-bearing mice treated with Peme and/or 4 Gy IR. (C) Tumor growth curves of xenograft-bearing mice treated with Peme and/or 2 Gy IR. *P<0.05, **P<0.01, ***P<0.001, ****P<0.0001. TGI, tumor growth inhibition; Peme, pemetrexed; TNBC, triple-negative breast cancer; NOD/SCID, non-obese diabetic/severe combined immunodeficiency; mpk, mg/kg; IR, ionizing radiation; CTRL, control; SC, subcutaneous.

exhibit reduced expression or functional instability, resulting in compromised DNA repair capacity and increased genomic instability (1,54,55). This clinical gap highlights the need for therapeutic strategies capable of restoring or stabilizing BRCA1 function in tumors with low BRCA1 activity.

CTSS serves as a critical regulator of BRCA1 stability by cleaving its BRCT domain and promoting ubiquitin-dependent degradation (12,14,23). CTSS inhibition effectively prevents BRCA1 proteolysis, providing a potential strategy to preserve BRCA1 integrity in TNBC. Building on this mechanistic insight, the present study conducted a high-throughput *in silico* screening of FDA-approved drugs to identify potential CTSS inhibitors. Peme was initially predicted to possess CTSS-inhibitory activity, however, subsequent CTSS

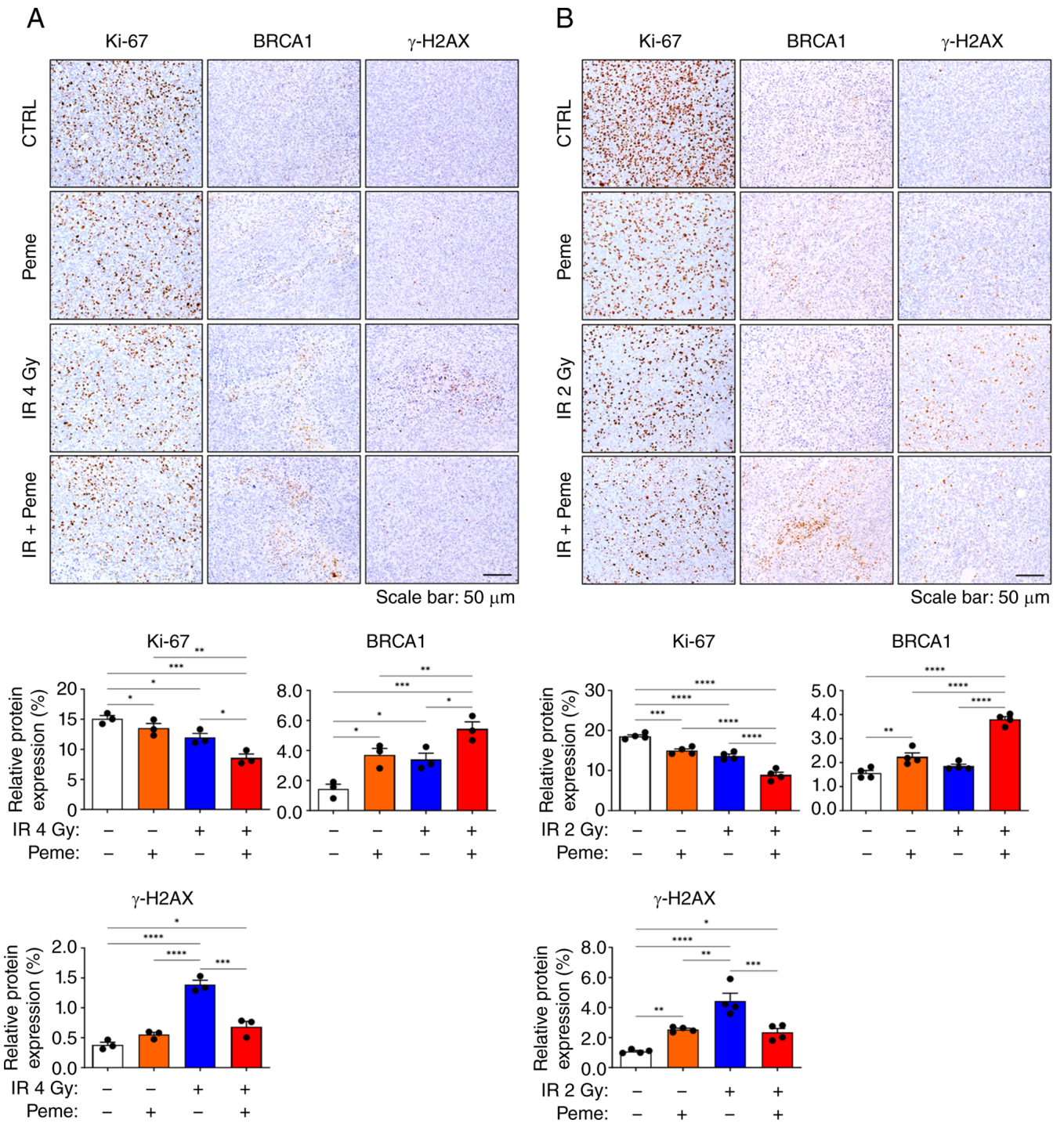

Figure 9. Peme promotes BRCA1-associated signaling in irradiated triple-negative breast cancer xenografts. (A) Immunohistochemical staining and quantification of Ki-67, BRCA1 and γ-H2AX in the 4 Gy xenograft groups. (B) Corresponding staining and quantification in the 2 Gy xenograft groups. Quantification of positive staining is presented as relative signal intensity. *P<0.05, **P<0.01, ***P<0.001, ****P<0.0001. Peme, pemetrexed; IR, ionizing radiation; CTRL, control.

enzymatic assays revealed that it exhibited only minimal CTSS inhibition compared with reference inhibitors. At the same time, Peme produced a greater increase in BRCA1 protein expression than the other screened candidate compounds in MDA-MB-231 cells without significant cytotoxicity, even at concentrations below the IC_{50} for CTSS inhibition. These findings suggested that Peme may regulate BRCA1 stability through mechanisms independent of direct CTSS inhibition.

To determine the biological relevance of Peme-induced BRCA1 upregulation, the present study investigated whether BRCA1 contributes to Peme-mediated cell death. Peme caused mild apoptosis, whereas combined treatment with Peme and IR resulted in enhanced BRCA1 expression and increased tumor cell death compared with either treatment alone. These results are consistent with the role of BRCA1 in facilitating apoptosis and orchestrating DNA damage response under genotoxic stress (8,56,57). Moreover, xenograft experiments confirmed that the combination of Peme and IR significantly delayed tumor growth and suppressed proliferation compared with IR-alone. The expression of BRCA1 and apoptosis markers was

also potentiated by Peme co-treatment. Together, these findings suggested that Peme may serve as a BRCA1-stabilizing radiosensitizer, enhancing therapeutic efficacy in TNBC. Clonogenic survival was evaluated under a limited IR condition rather than across a full IR dose-response range; additional studies are needed to clarify the radiosensitizing potential of Peme. Further studies using BRCA1-depleted or stable BRCA1-knockdown TNBC xenograft models are needed to more directly define the contribution of BRCA1 to the antitumor and radiosensitizing effects of Peme *in vivo*.

Beyond its canonical role in nuclear HR repair, BRCA1 also exerts cytoplasmic functions associated with mitotic regulation, mitochondrial homeostasis and apoptosis (1,52,58). DNA damage-induced cytotoxicity can be dissociated from BRCA1-mediated DNA repair and can depend on cytosolic BRCA1 accumulation (9,42,59). In addition, BRCA1 nuclear export following DNA damage is associated with increased cell susceptibility to genotoxic stress, supporting the hypothesis that BRCA1 function is influenced not only by its abundance but also by its subcellular localization (42,59). Consistent with these findings, our previous study showed that cytoplasmic BRCA1 stabilization is associated with apoptosis-related signaling, including BCL2 degradation, rather than with a canonical DNA repair response (23). In the present study, Peme-induced BRCA1 stabilization was accompanied by increased cytotoxicity, particularly when Peme was combined with IR. Therefore, the phenotype appears to be more consistent with apoptosis-associated cytosolic BRCA1 signaling than with enhancement of canonical nuclear HR repair. Nevertheless, a role of BRCA1-dependent DNA repair modulation cannot be excluded.

BRCA1 degradation is regulated by E3 ubiquitin ligases, including HERC2, HUWE1, FBXO44 and Parkin, as well as by caspase-3-mediated cleavage during apoptosis (1). The present results suggested that Peme interfered with the ubiquitin-proteasome degradation of BRCA1, potentially by stabilizing its C-terminal region. Consistent with the results obtained using BRCA1 deletion constructs, docking analysis suggested that the BRCT domain may contribute to the stabilizing effect of Peme on BRCA1. Specifically, Peme was predicted to occupy the phosphopeptide-binding region across the BRCT repeats, with a docking score comparable with that of the minimal phospho-tetrapeptide. However, because these observations were based on computational modeling and indirect functional evidence, they do not conclusively demonstrate a direct physical interaction between Peme and the BRCT domain. Therefore, the proposed involvement of the BRCT domain should be interpreted as a potential mechanistic model, and additional biochemical studies, such as cellular thermal shift assay or direct binding analyses, are required to validate this.

Clinically, Peme is already approved for the treatment of NSCLC and is well-tolerated in combination with radiotherapy (60,61). Given its favorable safety profile, repurposing Peme for TNBC therapy may be a feasible translational strategy. The ability of Peme to restore BRCA1 stability and potentiate IR-induced cytotoxicity offers a novel therapeutic possibility for patients with TNBC with wild-type but functionally deficient BRCA1. This approach not only broadens the clinical utility of Peme but also exemplifies the potential of targeted BRCA1 stabilization as a precision medicine strategy to overcome therapeutic resistance in TNBC.

Acknowledgements

Not applicable.

Funding

The present study was supported by the Basic Science Research Program (grant nos. RS-2025-00560618 and 2021R1A6C101A442) through the National Research Foundation of Korea funded by the Ministry of Science and ICT, the Ewha Womans University Research Grant (2024) and the RP-Grant 2025.

Availability of data and materials

The datasets used and analyzed during the current study are available from the corresponding author on reasonable request.

Authors' contributions

HJ edited the manuscript, designed and performed experiments and analyzed data. KHJ edited the manuscript, performed experiments and analyzed data. CK designed experiments and analyzed data. JL designed and performed experiments. YJL designed the study. YK edited the manuscript and conceived the study. YSL wrote and edited the manuscript and conceived the study. All authors have read and approved the final manuscript.

Ethics approval and consent to participate

All animal experiments were approved by the Institutional Animal Care and Use Committee of Ewha Womans University, Seoul, Republic of Korea (approval no. EWHA IACUC 23-049-t).

Patient consent for publication

Not applicable.

Competing interests

The authors declare that they have no competing interests.

References

1. Choi E, Mun GI, Lee J, Lee H, Cho J and Lee YS: BRCA1 deficiency in triple-negative breast cancer: Protein stability as a basis for therapy. Biomed Pharmacother 158: 114090, 2023.
2. Moser SC and Jonkers J: Thirty years of BRCA1: Mechanistic insights and their impact on mutation carriers. Cancer Discov 15: 461-480, 2025.
3. Gorodetska I, Kozeretska I and Dubrovska A: BRCA genes: The role in genome stability, cancer stemness and therapy resistance. J Cancer 10: 2109-2127, 2019.
4. Pleșea RM, Riza AL, Ahmet AM, Gavrilă I, Mituț A, Camen GC, Lungulescu CV, Dorobanțu Ș, Barbu A, Grigorescu A, *et al*: Clinically significant BRCA1 and BRCA2 germline variants in breast cancer-a single-center experience. Cancers (Basel) 17: 39, 2024.

5. Sharma P, Stecklein SR, Kimler BF, Sethi G, Petroff BK, Phillips TA, Tawfik OW, Godwin AK and Jensen RA: The prognostic value of BRCA1 promoter methylation in early stage triple negative breast cancer. J Cancer Ther Res 3: 1-11, 2014.
6. Yamashita N, Tokunaga E, Kitao H, Hitchins M, Inoue Y, Tanaka K, Hisamatsu Y, Taketani K, Akiyoshi S, Okada S, *et al*: Epigenetic inactivation of BRCA1 through promoter hypermethylation and its clinical importance in triple-negative breast cancer. Clin Breast Cancer 15: 498-504, 2015.
7. Irianiwati I, Gurky TC, Anwar SL, Bawono RG and Dwianingsih EK: Correlation between BRCA1 expression and the advanced stage of triple-negative breast cancer. Mol Clin Oncol 22: 32, 2025.
8. Thangaraju M, Kaufmann SH and Couch FJ: BRCA1 facilitates stress-induced apoptosis in breast and ovarian cancer cell lines. J Biol Chem 275: 33487-33496, 2000.
9. Montenegro MF, González-Guerrero R, Sánchez-Del-Campo L, Piñero-Madrona A, Cabezas-Herrera J and Rodríguez-López JN: PRMT1-dependent methylation of BRCA1 contributes to the epigenetic defense of breast cancer cells against ionizing radiation. Sci Rep 10: 13275, 2020.
10. Hedgepeth SC, Garcia MI, Wagner LE II, Rodriguez AM, Chintapalli SV, Snyder RR, Hankins GD, Henderson BR, Brodie KM, Yule DI, *et al*: The BRCA1 tumor suppressor binds to inositol 1,4,5-trisphosphate receptors to stimulate apoptotic calcium release. J Biol Chem 290: 7304-7313, 2015.
11. Lim JS, Lee KW, Ko KP, Jeong SI, Ryu BK, Lee MG and Chi SG: XAF1 destabilizes estrogen receptor α through the assembly of a BRCA1-mediated destruction complex and promotes estrogen-induced apoptosis. Oncogene 41: 2897-2908, 2022.
12. Choi E, Jeon KH, Lee H, Mun GI, Kim JA, Shin JH, Kwon Y, Na Y and Lee YS: Radiosensitizing effect of a novel CTSS inhibitor by enhancing BRCA1 protein stability in triple-negative breast cancer cells. Cancer Sci 115: 2036-2048, 2024.
13. Wu W, Koike A, Takeshita T and Ohta T: The ubiquitin E3 ligase activity of BRCA1 and its biological functions. Cell Div 3: 1, 2008.
14. Kim S, Jin H, Seo HR, Lee HJ and Lee YS: Regulating BRCA1 protein stability by cathepsin S-mediated ubiquitin degradation. Cell Death Differ 26: 812-825, 2019.
15. Wu W, Sato K, Koike A, Nishikawa H, Koizumi H, Venkitaraman AR and Ohta T: HERC2 is an E3 ligase that targets BRCA1 for degradation. Cancer Res 70: 6384-6392, 2010.
16. Lu Y, Li J, Cheng D, Parameswaran B, Zhang S, Jiang Z, Yew PR, Peng J, Ye Q and Hu Y: The F-box protein FBXO44 mediates BRCA1 ubiquitination and degradation. J Biol Chem 287: 41014-41022, 2012.
17. Wang X, Lu G, Li L, Yi J, Yan K, Wang Y, Zhu B, Kuang J, Lin M, Zhang S and Shao G: HUWE1 interacts with BRCA1 and promotes its degradation in the ubiquitin-proteasome pathway. Biochem Biophys Res Commun 444: 549-554, 2014.
18. Morris JR and Solomon E: BRCA1: BARD1 induces the formation of conjugated ubiquitin structures, dependent on K6 of ubiquitin, in cells during DNA replication and repair. Hum Mol Genet 13: 807-817, 2004.
19. Choudhury AD, Xu H and Baer R: Ubiquitination and proteasomal degradation of the BRCA1 tumor suppressor is regulated during cell cycle progression. J Biol Chem 279: 33909-33918, 2004.
20. Minten EV, Kapoor-Vazirani P, Li C, Zhang H, Balakrishnan K and Yu DS: SIRT2 promotes BRCA1-BARD1 heterodimerization through deacetylation. Cell Rep 34: 108921, 2021.
21. Miyahara K, Takano N, Yamada Y, Kazama H, Tokuhisa M, Hino H, Fujita K, Barroga E, Hiramoto M, Handa H, *et al*: BRCA1 degradation in response to mitochondrial damage in breast cancer cells. Sci Rep 11: 8735, 2021.
22. Yue X, Liu T, Wang X, Wu W, Wen G, Yi Y, Wu J, Wang Z, Zhan W, Wu R, *et al*: Pharmacological inhibition of BAP1 recruits HERC2 to competitively dissociate BRCA1-BARD1, suppresses DNA repair and sensitizes CRC to radiotherapy. Acta Pharm Sin B 13: 3382-3399, 2023.
23. Mun GI, Choi E, Jin H, Choi SK, Lee H, Kim S, Kim J, Kang C, Oh HL, Lee HJ, *et al*: Phosphorylation of BRCA1 at serine 1387 plays a critical role in cathepsin S-mediated radiation resistance via BRCA1 degradation and BCL2 stabilization. Biochim Biophys Acta Mol Basis Dis 1871: 167523, 2025.
24. Kim JL, Ha GH, Campo L and Breuer EK: Negative regulation of BRCA1 by transforming acidic coiled-coil protein 3 (TACC3). Biochem Biophys Res Commun 496: 633-640, 2018.
25. Hammond-Martel I, Pak H, Yu H, Rouget R, Horwitz AA, Parvin JD, Drobetsky EA and Affar el B: PI 3 kinase related kinases-independent proteolysis of BRCA1 regulates Rad51 recruitment during genotoxic stress in human cells. PLoS One 5: e14027, 2010.
26. Murai J, Huang SY, Das BB, Renaud A, Zhang Y, Doroshow JH, Ji J, Takeda S and Pommier Y: Trapping of PARP1 and PARP2 by clinical PARP inhibitors. Cancer Res 72: 5588-5599, 2012.
27. Lin Z, Wang L, Xing Z, Wang F and Cheng X: Update on combination strategies of PARP inhibitors. Cancer Control 31: 10732748241298329, 2024.
28. Shih C, Chen VJ, Gossett LS, Gates SB, MacKellar WC, Habeck LL, Shackelford KA, Mendelsohn LG, Soose DJ, Patel VF, *et al*: LY231514, a pyrrolo[2,3-d]pyrimidine-based antifolate that inhibits multiple folate-requiring enzymes. Cancer Res 57: 1116-1123, 1997.
29. Adjei AA: Pemetrexed (Alimta): A novel multitargeted antifolate agent. Expert Rev Anticancer Ther 3: 145-156, 2003.
30. Schneeweiss A, Marmé F, Ruiz A, Manikhas AG, Bottini A, Wolf M, Sinn HP, Mansouri K, Kennedy L and Bauknecht T: A randomized phase II trial of doxorubicin plus pemetrexed followed by docetaxel versus doxorubicin plus cyclophosphamide followed by docetaxel as neoadjuvant treatment of early breast cancer. Ann Oncol 22: 609-617, 2011.
31. O'Shaughnessy JA, Clark RS, Blum JL, Mennel RG, Snyder D, Ye Z, Liepa AM, Melemed AS and Yardley DA: Phase II study of pemetrexed in patients pretreated with an anthracycline, a taxane, and capecitabine for advanced breast cancer. Clin Breast Cancer 6: 143-149, 2005.
32. Wan F, Chen X, Dong LF, Cheng YH and Long JP: A systemic analysis on pemetrexed in treating patients with breast cancer. Asian Pac J Cancer Prev 15: 4567-4570, 2014.
33. Bai F, Yin Y, Chen T, Chen J, Ge M, Lu Y, Xie F, Zhang J, Wu K and Liu Y: Development of liposomal pemetrexed for enhanced therapy against multidrug resistance mediated by ABCC5 in breast cancer. Int J Nanomedicine 13: 1327-1339, 2018.
34. Leonetti A, Baroli G, Fratini E, Pietropaoli S, Marcoli M, Mariottini P and Cervelli M: Epileptic seizures and oxidative stress in a mouse model over-expressing spermine oxidase. Amino Acids 52: 129-139, 2020.
35. Fu JF, Shih LY and Yen TH: HOXA11 plays critical roles in disease progression and response to cytarabine in AML. Oncol Rep 46: 150, 2021.
36. Zhai Z, Zhang X, Ding Y, Huang Z, Li Q, Zheng M, Cho K, Dong Z, Fu W, Chen Z and Jiang B: Eugenol restrains abdominal aortic aneurysm progression with down-regulations on NF-κB and COX-2. Phytother Res 36: 928-937, 2022.
37. Sungeelee S, Mailhes-Hamon C, Chettouh Z, Bokiniec P, Eymael A, McMullan S, Léna C, Dempsey B and Brunet JF: A genetically defined pontine nucleus essential for ingestion in mice. Proc Natl Acad Sci USA 122: e2411174122, 2025.
38. Rakhmilevich AL, Tsarovsky NW, Felder M, Zaborek J, Moram S, Erbe AK, Pieper AA, Spiegelman DV, Cheng EM, Witt CM, *et al*: A combined radio-immunotherapy regimen eradicates late-stage tumors in mice. Front Immunol 15: 1419773, 2024.
39. Zagorac I, Ramírez-Fernández Á, Tapia-Galisteo A, Rubio-Pérez L, Gómez-Rosel M, Grau M, Rodríguez-Peralto JL, Álvarez-Vallina L and Blanco B: mRNA-engineered T lymphocytes secreting bispecific T cell engagers with therapeutic potential in solid tumors. Front Immunol 16: 1684655, 2025.
40. Rupanagudi KV, Kulkarni OP, Lichtnekert J, Darisipudi MN, Mulay SR, Schott B, Gruner S, Haap W, Hartmann G and Anders HJ: Cathepsin S inhibition suppresses systemic lupus erythematosus and lupus nephritis because cathepsin S is essential for MHC class II-mediated CD4 T cell and B cell priming. Ann Rheum Dis 74: 452-463, 2015.
41. Wei L, Shao N, Peng Y and Zhou P: Inhibition of cathepsin S restores TGF-β-induced epithelial-to-mesenchymal transition and tight junction turnover in glioblastoma cells. J Cancer 12: 1592-1603, 2021.
42. Wang H, Yang ES, Jiang J, Nowsheen S and Xia F: DNA damage-induced cytotoxicity is dissociated from BRCA1's DNA repair function but is dependent on its cytosolic accumulation. Cancer Res 70: 6258-6267, 2010.
43. Na Z, Pan S, Uttamchandani M and Yao SQ: Discovery of cell-permeable inhibitors that target the BRCT domain of BRCA1 protein by using a small-molecule microarray. Angew Chem Int Ed Engl 53: 8421-8426, 2014.

44. Periasamy J, Kurdekar V, Jasti S, Nijaguna MB, Boggaram S, Hurakadli MA, Raina D, Kurup LM, Chintha C, Manjunath K, *et al*: Targeting phosphopeptide recognition by the human BRCA1 tandem BRCT domain to interrupt BRCA1-dependent signaling. Cell Chem Biol 25: 677-690.e12, 2018.
45. Duriez PJ and Shah GM: Cleavage of poly(ADP-ribose) polymerase: A sensitive parameter to study cell death. Biochem Cell Biol 75: 337-349, 1997.
46. Porter AG and Jänicke RU: Emerging roles of caspase-3 in apoptosis. Cell Death Differ 6: 99-104, 1999.
47. Wu J, Lu LY and Yu X: The role of BRCA1 in DNA damage response. Protein Cell 1: 117-123, 2010.
48. Savage KI and Harkin DP: BRCA1, a 'complex' protein involved in the maintenance of genomic stability. FEBS J 282: 630-646, 2015.
49. Jin S, Zhao H, Fan F, Blanck P, Fan W, Colchagie AB, Fornace AJ Jr and Zhan Q: BRCA1 activation of the GADD45 promoter. Oncogene 19: 4050-4057, 2000.
50. Agelidis A, Ter-Zakarian A and Jaloudi M: Triple-negative breast cancer on the rise: Breakthroughs and beyond. Breast Cancer (Dove Med Press) 17: 523-529, 2025.
51. Jie H, Ma W and Huang C: Diagnosis, prognosis, and treatment of triple-negative breast cancer: A review. Breast Cancer (Dove Med Press) 17: 265-274, 2025.
52. Arun B, Couch FJ, Abraham J, Tung N and Fasching PA: BRCA-mutated breast cancer: The unmet need, challenges and therapeutic benefits of genetic testing. Br J Cancer 131: 1400-1414, 2024.
53. Desnoyers A, Nadler M, Wilson BE, Stajer S and Amir E: Associations with response to Poly(ADP-ribose) Polymerase (PARP) inhibitors in patients with metastatic breast cancer. NPJ Breast Cancer 8: 43, 2022.
54. Raimundo L, Calheiros J and Saraiva L: Exploiting DNA damage repair in precision cancer therapy: BRCA1 as a prime therapeutic target. Cancers (Basel) 13: 3438, 2021.
55. Sellars E, Savguira M, Wu J, Cancelliere S, Jen M, Krishnan R, Hakem A, Barsyte-Lovejoy D, Hakem R, Narod SA, *et al*: A high-throughput approach to identify BRCA1-downregulating compounds to enhance PARP inhibitor sensitivity. iScience 27: 110180, 2024.
56. Sadeghi F, Asgari M, Matloubi M, Ranjbar M, Karkhaneh Yousefi N, Azari T and Zaki-Dizaji M: Molecular contribution of BRCA1 and BRCA2 to genome instability in breast cancer patients: Review of radiosensitivity assays. Biol Proced Online 22: 23, 2020.
57. Li Q, Qian W, Zhang Y, Hu L, Chen S and Xia Y: A new wave of innovations within the DNA damage response. Signal Transduct Target Ther 8: 338, 2023.
58. Chen Q, Lei JH, Bao J, Wang H, Hao W, Li L, Peng C, Masuda T, Miao K, Xu J, *et al*: BRCA1 deficiency impairs mitophagy and promotes inflammasome activation and mammary tumor metastasis. Adv Sci (Weinh) 7: 1903616, 2020.
59. Jiang J, Yang ES, Jiang G, Nowsheen S, Wang H, Wang T, Wang Y, Billheimer D, Chakravarthy AB, Brown M, *et al*: p53-dependent BRCA1 nuclear export controls cellular susceptibility to DNA damage. Cancer Res 71: 5546-5557, 2011.
60. Li J and Xu X: Application of pemetrexed for the treatment of non-small-cell lung cancer. J Int Oncol: 123-126, 2013.
61. Citarella F, Russano M, Galletti A, Di Fazio GR, Vincenzi B, Tonini G and Santini D: Effectiveness of pemetrexed-based chemotherapy and radiation therapy in RET-rearranged lung adenocarcinoma: A mono-institutional case series. Precis Cancer Med 4: 17, 2021.